Hydrogen adsorption on sp^2-bonded carbon: Influence of the local curvature

P. Ruffieux,[1,*] O. Gröning,[1,2] M. Bielmann,[1] P. Mauron,[1] L. Schlapbach,[1,2] and P. Gröning[1]
[1]*Physics Department, University of Fribourg, Pérolles, CH-1700 Fribourg, Switzerland*
[2]*Swiss Federal Laboratories for Materials Testing and Research, Überlandstrasse 129, 8600 Dübendorf, Switzerland*
(Received 19 July 2002; published 20 December 2002)

The interaction of atomic hydrogen and low-energy hydrogen ions with sp^2-bonded carbon is investigated on the surfaces of C_{60} multilayer films, single-walled carbon nanotubes, and graphite (0001). These three materials have been chosen to represent sp^2-bonded carbon networks with different local curvatures and closed surfaces (i.e. no dangling bonds). Chemisorption of hydrogen on these surfaces reduces emission from photoemission features associated with the π electrons and leads to a lowering of the work function up to 1.3 eV. It is found that the energy barrier for hydrogen adsorption decreases with increasing local curvature of the carbon surface. Whereas in the case of C_{60} and single-walled carbon nanotubes, hydrogen adsorption can be achieved by exposure to atomic hydrogen, the hydrogen adsorption on graphite (0001) requires H^+ ions of low kinetic energy ($\sim$1 eV). On all three materials, the adsorption energy barrier is found to increase with coverage. Accordingly, hydrogen chemisorption saturates at coverages that depend on the local curvature of the sample and the form of hydrogen (i.e., atomic or ionic) used for the treatment.

DOI: 10.1103/PhysRevB.66.245416 PACS number(s): 68.43.−h, 71.20.Tx, 81.07.De

I. INTRODUCTION

Adsorbates, topological defects, and atomic vacancies influence many physical properties of solids and modify the electronic structure, particularly for nanosized systems.[1–3] Scanning tunneling microscopy has been used to image the long-range ($\sim$6 nm) modifications in the electronic structure of sp^2-bonded carbon networks caused by hydrogen adsorption sites, atomic vacancies and structural defects.[4–7] Recently, defects acting as tunnel barriers or as electron scatterers have been used for the realization of electronic devices on single carbon nanotubes.[1,3] Chemisorption of hydrogen on sp^2-bonded carbon is an interesting candidate for the local modification of the electronic structure since it leads to a local rehybridization from sp^2 to sp^3 of the carbon network.

Additional interest in the interaction of hydrogen with graphitic surfaces originates from the astrophysical community. Interstellar dust particles containing graphite are thought to play a catalytic role for the H_2 formation from atomic hydrogen in interstellar space. The yield of different recombination mechanisms strongly depends on the binding energy, the mobility, and the potential barriers of hydrogen atoms on graphitic surfaces and has therefore led to several theoretical investigations of the hydrogen-graphite system.[8,9]

The chemical binding of hydrogen to an sp^2-bonded carbon network requires a local rehybridization from sp^2 to sp^3 and has therefore a rather large adsorption energy barrier for a strictly planar sp^2-bonded carbon network. Figure 1 shows the calculated potential energy for a hydrogen atom approaching a graphite surface where all carbon atoms are fixed to positions in the same plane and further for a graphite surface where one carbon atom is fixed at 0.36 Å above the plane defined by its neighbors, as presented by Sha and Jackson.[9] The almost complete reduction of the adsorption energy barrier for the carbon atom raised by 0.36 Å shows a strong dependence of the energy barrier on the local tetrahedrezation, i.e., the admixture of sp^3 character to the sp^2 configuration. Starting from these considerations, the adsorption energy barrier should strongly depend on local deviations from planarity of sp^2-bonded structures. More precisely, the adsorption energy barrier is expected to be lower for convex structures due to an increased sp^3 character introduced by the local curvature.

In this work, we investigated the interaction of atomic hydrogen with sp^2-bonded carbon as a function of the local curvature of the graphitic network. In order to cover a large range of curvature, we chose graphite (0001), single-walled carbon nanotubes (SWNT's), and C_{60} fullerenes as substrates. The radius of curvature ranges from $r=\infty$ for graphite to $r=3.55$ Å for C_{60}.

The paper is organized as follows. Details on the sample preparation and on the hydrogen sources used for the treat-

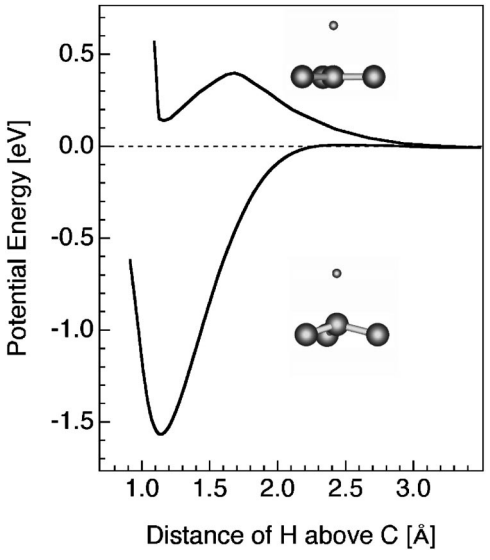

FIG. 1. Interaction potential as a function of hydrogen-substrate distance as calculated by Sha and Jackson (Ref. 9) for top-site adsorption. The upper curve shows the result for flat geometry. The lower curve shows the potential for a protruded (0.36 Å) carbon atom.

ments are given in the experimental section. In the following section we first discuss the results of the individual samples followed by a discussion of the interaction of hydrogen with sp^2-bonded carbon from the point of view of the local curvature of the samples.

II. EXPERIMENT

Experiments were performed in an OMICRON photoelectron spectrometer modified for motorized sequential angle-scanning data acquisition having a base pressure in the range of 5×10^{-11} mbar. The analysis part is equipped with a twin-anode x-ray source (Mg $K\alpha$, $h\nu=1253.6$ eV; Al $K\alpha$, $h\nu=1486.7$ eV) for x-ray photoelectron spectroscopy (XPS) and a He discharge lamp (He I: $h\nu=21.2$ eV; He II: $h\nu=40.8$ eV) for ultraviolet photoelectron spectroscopy (UPS). The connected preparation chamber has been extended with an electron cyclotron resonance (ECR) microwave plasma source and an atomic hydrogen source.

Typical plasma treatments were conducted at a hydrogen pressure of 10^{-2} mbar and a microwave power of 60 W with the sample positioned at a distance of about 6 cm from the ECR-plasma region. The ion energy distribution has been determined using an electrostatical analyzer.[10,11] Spectra taken under the conditions used in the following experiments show that 85% of the hydrogen ions are in a narrow energy region around 1 eV and the maximum detected energy is $\sim$16 eV. A typical ion flux at the sample position is of the order of 2×10^{13} s^{-1} cm^{-2}.

The atomic hydrogen source has been built with the design proposed by Bischler and Bertel,[12] where the hydrogen molecules are dissociated in a heated tungsten tube (1700 °C), through which the hydrogen is dosed onto the sample. The design enables high dissociation efficiencies of about 50% (at 1700 °C) and allows fluxes of atomic hydrogen of $\sim10^{14}$ s^{-1} cm^{-2} at the sample position with a background pressure of 3×10^{-8} mbar.

The C_{60} film ($\sim$40 Å) has been grown on a clean and well-ordered Cu(111) surface by evaporation from a resistively heated stainless steel crucible. The film has been judged well ordered based on low-energy electron diffraction (LEED).

For the investigations on SWNT's we used fullerene samples that were produced out of commercially available SWNT's (Tubes@Rice, Carbon Nanotechnologies, Inc.). Samples were cleaned *in situ* by heating to 800 °C for several hours. The cleanliness of the samples was checked with XPS revealing contamination free ($<$1 at %) surfaces. Raman analysis of the nanotube samples has been performed on a commercial microspectrometer (Labram, Dilor) under ambient conditions using a green excitation laser (514.5 nm).

The single-crystal graphite sample [C(0001)] has been cleaved under UHV conditions and heated to 800 °C for several hours. The surface has been judged clean and well ordered based on XPS and LEED measurements.

III. RESULTS AND DISCUSSION

A. H/C_{60}

Figure 2 shows a series of valence band spectra of a C_{60} multilayer film taken for different H_2 plasma treatment times. Spectra were measured on a 40 Å mulilayer film on Cu(111) using He II radiation (40.8 eV) and normalized to have the same integrated intensity with respect to the range of 0–17 eV binding energy. The energy transferred from the hydrogen ions to the C_{60} molecules is limited to a level that is low enough to prevent molecule desorption during plasma treatments, as has been checked with XPS where no film thickness variation was detected.

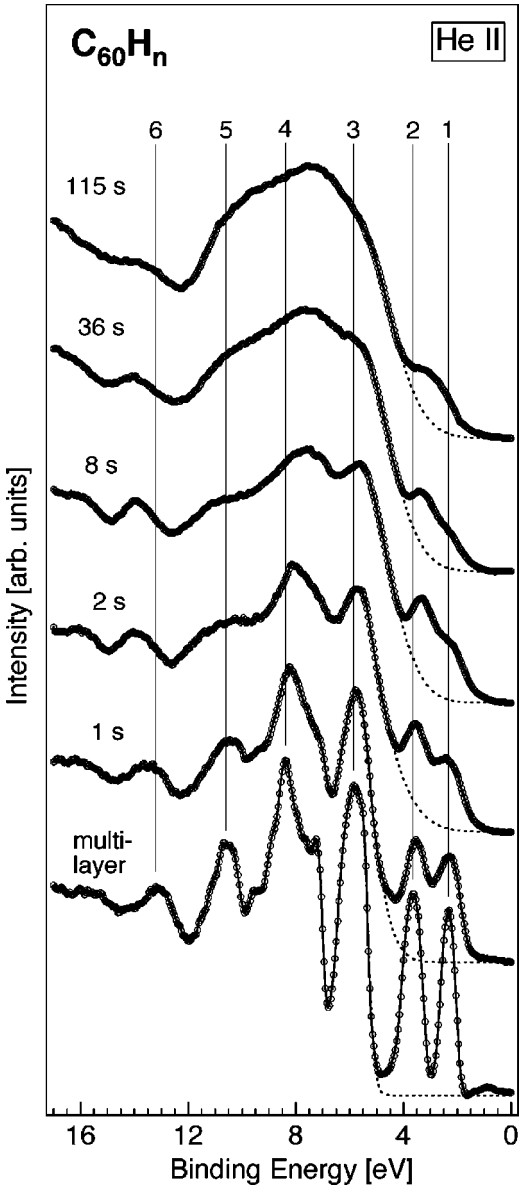

FIG. 2. Series of valence band spectra for different H_2 plasma treatment times measured using He II radiation (40.8 eV) and an energy resolution of 200 meV. The valence band spectra are normalized to the integrated intensity between 0 and 17 eV binding energy and are displayed with an offset. The background below the features 1 and 2 has been determined by fitting a Gauss tail to feature 3.

The bottom curve shows the valence band of the untreated film with the highest occupied orbital (HOMO) located at 2.3 eV. The HOMO and the HOMO-1, labeled 1 and 2, are pure

π orbitals.[15] They have degeneracies of 10 and 18, respectively, and are thus occupied by 28 electrons. States with binding energies >4 eV are of mixed σ-π character.

Exposing the C_{60} multilayer film to H_2 plasma results in a marked intensity reduction on the features labeled 1 and 2. At the same time the spectral features shift by up to 0.9 eV (feature 4). The observation of features shifted in the opposite direction indicates that the shifts are not due to a Fermi level shift, i.e., due to doping of the film. The strongest increase in intensity is observed at a binding energy of ~10 eV.

The intensity reduction on the two highest occupied orbitals and the intensity gain on states with higher binding energies indicates the conversion of delocalized π states to C-H bond states with σ character, which have a binding energy of ~10 eV.[16,17] The intensity reduction gives a measure of how many of the 28 π electrons contained in the two highest molecular orbitals are converted to lower-lying C-H bonds. The maximum reduction of intensity observed on the π-derived states is 73% (intensity determination after background substraction), indicating the conversion of ~20 π electrons. However, this estimation does not take into account the conversion of lower-lying π states. Assuming a similar reduction as on the pure π states results in a conversion of ~44 π electrons in all. This indicates a somewhat higher degree of hydrogenation as has been synthesized via a Birch reduction, yielding $C_{60}H_{36}$.[13,14] Theoretical results show that $C_{60}H_{36}$ and $C_{60}H_{48}$ are very stable molecules.[18] Further hydrogenation is energetically unfavorable due to the increased stress in the molecule induced by the sp^2 to sp^3 rehybridization. Another limiting factor may be stress induced by the expected lattice expansion when hydrogen is adsorbed on the fullerenes, since in this experiment hydrogenation is done on a solid film and not on free molecules.

Hydrogenation of the C_{60} films results in an important lowering of the work function, as seen on the position of the low-energy cutoff of the valence band spectrum [Fig. 3(a)]. For the longest treatment time, the work function amounts to 3.6 eV, which signifies a drastic lowering by 1.3 eV compared to the as-deposited C_{60} film. The lower work function indicates a change in the surface dipole originating from the polar C-H bond. Since hydrogen atoms are adsorbed on the outside of the fullerene cage and carbon is the more electronegative element, a dipole layer is formed at the surface with the positive charge on the vacuum side. This lowering of the work function induced by hydrogen chemisorption has been observed on other carbon allotropes and is in particular responsible for the negative electron affinity at diamond surfaces.[4,19]

The main change observed in the XPS study is an increasing linewidth of the C 1*s* line upon hydrogen uptake in the C_{60} film. Figure 3(b) shows the spectrum of the C1*s* core level for the C_{60} multilayer film before and after 36 s of H_2 plasma treatment. The line broadens to higher binding energies resulting in an increase of the full width at half maximum (FWHM) from 0.8 eV to 1.1 eV and a shift of the peak position from 284.48 eV to 284.55 eV, as determined from a fit to the data. This contribution at higher binding energies is known to be the C-H component, although electronegativity

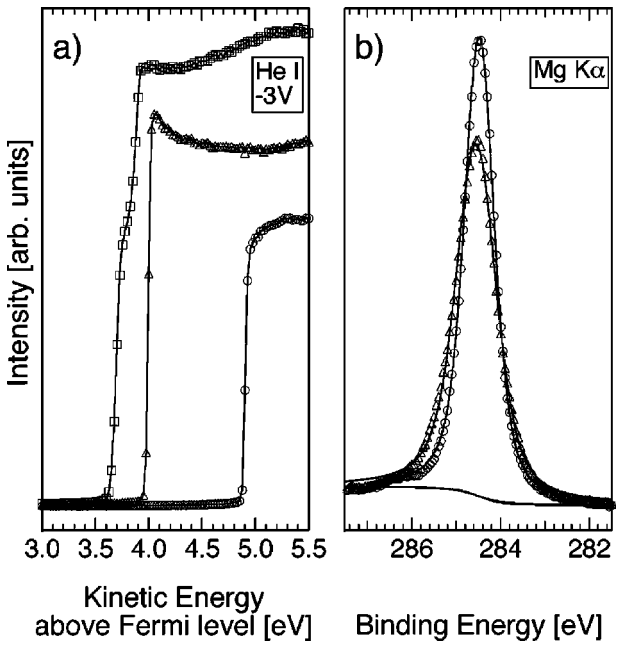

FIG. 3. (a) Low-energy cutoff of the valence band of C_{60} measured with He I radiation (21.2 eV) and an energy resolution of 30 meV for the untreated film (circles), after 36 s (triangles), and 115 s (squares) plasma treatment. The sample was biased to −3 V in order to overcome the work function of the electron analyzer. The energy scale has been corrected for the applied sample bias and displays the energy with respect to the Fermi level. The work function has been determined by taking the intersection of the intensity cutoff with the energy axis at zero intensity. (b) C 1*s* core level spectra excited with Mg $K\alpha$ measured before (circles) and after 36 s (triangles) H_2 plasma. Spectra were recorded in normal emission and have been normalized to total intensity after background substraction.

arguments would yield a shift to the opposite direction, since carbon is the more electronegative element. The shift to higher binding energies has to be explained by a different relaxation energy of the differently hybridized carbon atoms, as has been shown for different hydrocarbon systems.[20–22] Part of the broadening may also be due to the larger depth that is probed by XPS (~50 Å) compared to the UPS study, which is sensitve to the outermost molecule layer only.

The same series of measurements has been performed on C_{60} films that were exposed to atomic hydrogen. The second spectrum in Fig. 4 shows the valence band of the C_{60} multilayer film for a treatment level, where the hydrogen uptake has saturated. The intensity on the pure π states is lowered to 47% of the value for the untreated sample, which is in agreement with the results presented by Ohno *et al.*[23] This indicates a conversion of ~28 π states if a similar reduction on the lower-lying π states is assumed, as discussed above. The lowering of the work function amounts to ~0.8 eV. Comparison with the valence band spectrum of the C_{60} film that was exposed to H_2 plasma shows that the evolution of spectral features upon hydrogenation is identical for plasma and atomic hydrogen treatments. This further confirms that damage induced by hydrogen ions can be neglected at least for plasma treatments up to this level.

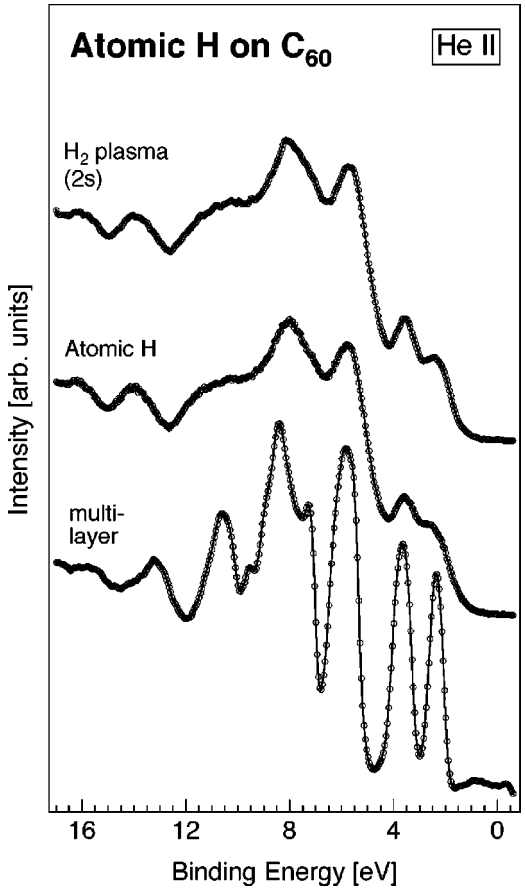

FIG. 4. Valence band spectra of the C_{60} film after different treatments. The spectrum at the bottom shows the valence band for the untreated film. The second spectrum shows the spectrum for the atomic hydrogen treated film after a treatment time of where hydrogen chemisorption has reached its saturation value. The top spectrum shows the valence band after a H_2 plasma treatment of 2 s, yielding similar changes as for the saturation coverage of atomic hydrogen.

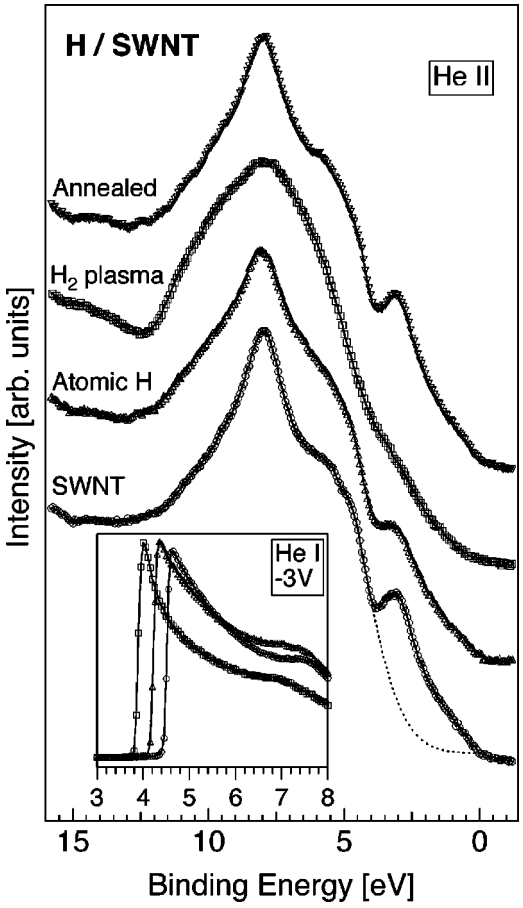

FIG. 5. Valence band spectra of SWNT's for the untreated (circles), atomic-hydrogen-treated (triangles), and plasma-treated (squares) sample using He II radiation (40.8 eV). Spectra have been offset for better visibility. The intensity on the π-derived states has been determined after substraction of a Gauss background (dotted line). The inset shows the low-energy cutoff of the valence band as a function of kinetic energy relative to the Fermi level. These spectra have been measured with a sample bias of -3 V.

Since H_2 plasma contains both reactive species, atomic hydrogen and hydrogen ions, the higher level of hydrogenation achieved with the plasma can be attributed to the presence of the hydrogen ions. At the level where hydrogen uptake saturates for treatments with atomic hydrogen, the hydrogen ions still see an adsorption energy barrier that is sufficiently low to allow further hydrogenation of the C_{60} film.

B. H/SWNT

SWNT's can be looked at as rolled up graphene sheets resulting in tubules with diameters of $d_T \geq 4$ Å,[24] where the electronic properties approach those of graphene with increasing diameter. States with a binding energy less than $\sim$4 eV are of pure π character, whereas states in the range of 4 to 11 eV have mixed σ-π character and states having binding energies larger than $\sim$11 eV are pure σ states.

We have used Raman spectroscopy to determine the diameter of the SWNT samples. It has been shown that the position of the first spectral feature in the Raman spectrum, the radial breathing mode, observed between 140 and 220 cm^{-1}, is unique for SWNT.[25] For the laser line used in this work (514.5 nm), the wave number ν of the radial breathing mode is, to a good approximation, related to the tube diameter d_T as $1/d_T = \nu/234$, and thus allows the determination of the mean tube diameter of the sample.[25] Analysis of the SWNT (Tubes@Rice) used for this study revealed a mean tube diameter of $d_T \simeq 1.2$ nm.

Figure 5 displays valence band spectra of the SWNT film measured using He II radiation (40.8 eV). The prominent spectral features observed for the untreated SWNT film are similar to those observed in angle-integrated measurements on graphite. The state at $\sim$2.5 eV binding energy is a pure π state and thus represents a feature whose intensity is supposed to be lowered in intensity if hydrogen is chemically bond to the tube walls since in that case, as discussed above, the delocalized π states are transformed to lower lying C-H states. In contrast to this, the passivation of dangling bonds of carbon atoms at the edge of graphene sheets, as for open tubes or tube fragments, with hydrogen does not affect the π

states, since this C-H bond state is a σ state and does not mix with the π states.[26] The work function of the untreated film is 4.4 eV, as determined from the low-energy cutoff of the He I spectrum.

In order to be able to distinguish between hydrogenation induced by atomic hydrogen and hydrogen ions, we first treated the film with atomic hydrogen. The second spectrum in Fig. 5 shows the valence band after 120 s of treatment with atomic hydrogen. At this level of atomic hydrogen treatment the reduction on the intensity of the π-derived states has achieved its saturation value of ~22% and the work function has been lowered by 0.3 eV to 4.1 eV (inset of Fig. 5). This shows a significant hydrogen uptake on this type of tubes, but remains significantly below the value observed for the atomic hydrogen treatment of the C_{60} film (47%).

Further hydrogenation of the SWNT film could be achieved by H_2 plasma treatment. This is manifested by a further reduction of the spectral weight of states with binding energies <4 eV. Hydrogen uptake seems to saturate after 200 s of plasma treatment when the intensity of the π-derived states has been reduced to ~50% of its original value, i.e., half of the delocalized π states have been transformed to lower lying C-H states resulting in a coverage of $\theta \simeq 0.5$ of chemisorbed hydrogen. Similar to the C_{60} film, these new states are located at ~10 eV binding energy. This further hydrogen uptake results in a work function of 3.8 eV, which is 0.6 eV lower than that for the untreated film. However, uncertainty remains about the hydrogen coverage of the nanotubes, since these samples are known to contain small amounts of amorphous carbon residues, which may contribute to the spectral weight on the π states.

XPS analysis on the films shows a similar behavior as observed on the C_{60} film. Hydrogen uptake gives rise to a new component at higher binding energies, leading to an increase of the FWHM from 1.05 eV to 1.14 eV for the sample exposed to atomic hydrogen.

Heating the samples to ~800 °C restores the original valence band and the work function of 4.4 eV, indicating that all hydrogen has desorbed at this temperature and that damage on the tubes induced by the most energetic hydrogen ions is limited to a low level.

Lee and co-workers predicted two stable configurations of hydrogenated SWNT's with a coverage of $\theta=1$ based on a density functional calculation.[27,28] The *zigzag* type has hydrogen atoms alternatively chemisorbed on the inside and on the outside of the tube wall and has a higher stability than the *arch* type, which has all the hydrogen atoms at the exterior of the tube wall. The superior stability of the *zigzag* type is due to a more pronounced tetrahedrization that is allowed by the alternating position of the hydrogen atoms with respect to the tube wall.

The observed lowering of the work function does not speak in favor of the *zigzag* geometry since for this adsorbate configuration, no pronounced change of the surface dipole is expected due to the position of the hyrogen atoms, which adsorb alternatively on the inside and the outside of the tube wall. On the other hand, chemisorption on the outside of the tube wall agrees well with the observed change in surface dipole. However, the coverage seems to be limited to $\theta \simeq 0.5$ even with hydrogen ions having an energy of ~1 eV. A possible explanation of this limiting behavior is an adsorption energy barrier that increases with hydrogen coverage. This can be understood by taking into account the pull-out of the carbon atom induced by the C-H bond formation.[9] This results in an increased energy barrier for hydrogen chemisorption on the neighbor atoms, since the latter find themselves in a depressed position. If this larger adsorption energy barrier is too high for the bond formation, the maximum coverage will be limited to $\theta=0.5$ with hydrogen chemisorbed to every second carbon atom.

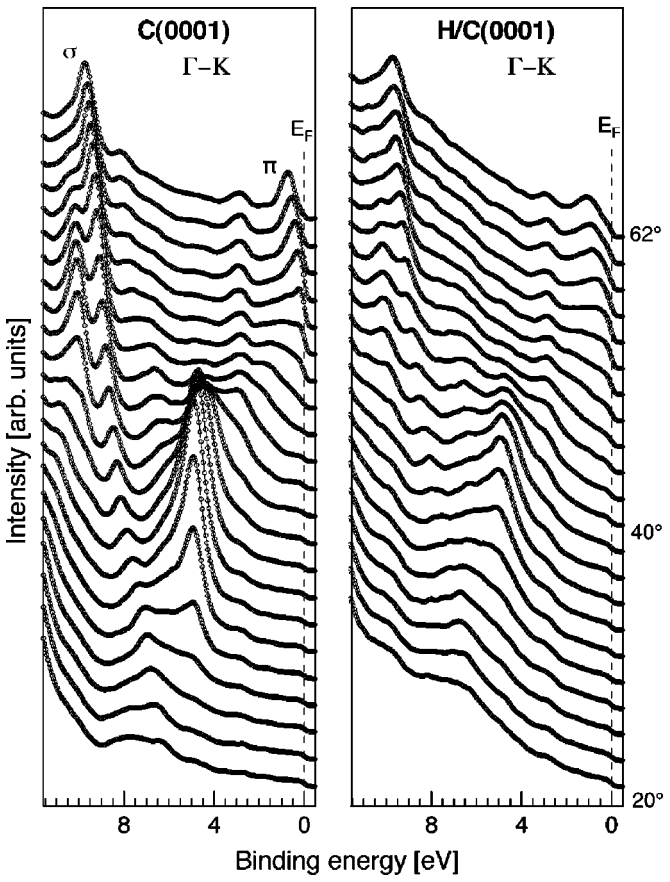

FIG. 6. Angle-resolved spectra in the $\Gamma-K$ direction for the untreated C(0001) surface and after 180 s H_2 plasma treatment using He I (21.2 eV) radiation and an energy resolution of 60 meV. Spectra are taken for polar angles in the range between 62° and 20° with increments of 2°.

C. H/Graphite

Figure 6 shows uv photoemission spectra of the C(0001) surface taken for different polar emission angles ϑ along the $\Gamma-K$ direction of the Brioullin zone direction using He I radiation (21.2 eV). The angle-resolved measurements allow a clear attribution of the photoelectron features to the various valence bands of graphite. Spectra in the $\Gamma-K$ direction are dominated by two dispersing features, which are due to emission from a σ band at high binding energies and emission from the π band dispersing from the Fermi level ($\vartheta=54°$) to 5 eV binding energy ($\vartheta=34°$), respectively. The

low-energy cutoff of the valence band spectrum reveals a work function of 4.5 eV for the untreated sample.

In a first attempt to adsorb hydrogen on the graphite surface we exposed the sample to atomic hydrogen. Comparison of the electronic structure and the work function with the values before the treatment showed no change induced by the atomic hydrogen. That is even the case for doses where hydrogen chemisorption has saturated on C_{60} and SWNT's.

The situation is different when the C(0001) surface is treated in the H_2 plasma. Doses of about 10^{14} ions/cm^2 cause modifications in the electronic structure of the surface. The intensity on the π band decreases as a function of the plasma treatment time. The ratio between the intensity on the π state and the intensity on the σ state drops by a factor of about 1.7 for the longest treatment time (390 s). This indicates that the hydrogen ions are sufficiently energetic to chemically bond to the basal plane of graphite. Hydrogen adsorption leads to a broadening of the features, which affects especially the π band. The σ-derived state shows an increase of the FWHM from 0.79 to 0.84 eV, whereas the FWHM of the π-derived state increases from 0.63 to 0.86 eV (Fig. 6). At 9.9 eV binding energy, a localized state appears upon hydrogen uptake at the surface. The dispersing graphitic features remain unchanged in their energy position.

Spectra taken in the $\Gamma - M$ direction are dominated by a single dispersing feature at 8–3 eV binding energy, which is due to emission from a π band. The changes due to hydrogen uptake are similar to the ones observed on the π band in the $\Gamma - K$ direction, i.e., a lowering of the intensity and a small broadening. Again, a hydrogen-related state appears at 9.9 eV binding energy with increasing coverage of chemisorbed hydrogen.

Chemisorption of hydrogen leads to an increased emission of secondary electrons over the hole range of the valence band and the lowering of the work function by 0.4 eV to a value of 4.1 eV for a treatment time of 390 s (Fig. 7). The nondispersing feature at 9.9 eV binding energy is consistent with the position of the hydrogen-related feature of density-of-states calculations for this C-H configuration.[16]

XPS analysis at grazing emission (enhanced surface sensitivity) of the C 1*s* core level after different treatment times shows the growing of a hydrogen-related component at higher binding energies leading to a broadening of the line by ~0.1 eV.

For the longest treatment times a loss of surface quality was observed in the LEED pattern. This is due to the small fraction of hydrogen ions having an energy that is high enough to create atomic vacancies in the top layer, as observed with atomic force microscopy.[4] This might also be responsible for part of the broadening observed on the spectral features.

The theoretical works of Jeloaica and Sidis[8] and Sha and Jackson[9] showed density functional theory (DFT) calculations of the potential energy between atomic hydrogen and the graphite surface. They found adsorption energy barriers of ~0.2 eV for an approaching hydrogen atom in the case where the carbon atom below the hydrogen atom is allowed to fully relax to its minimum energy position. However, a substantial displacement of ~0.4 Å is required to minimize the energy barrier. If the carbon atoms are not allowed to move, the adsorption energy barrier ''seen'' by the hydrogen atom increases to ~0.4 eV. The theoretical works thus yields an energy barrier for the chemisorption process that varies between ~0.2 eV and ~0.4 eV, depending on how fast the carbon atoms can relax. However, the experimental results show that thermally dissociated hydrogen does not chemisorb on the graphite surface. This indicates that the calculated adsorption energy barriers are probably underestimated.

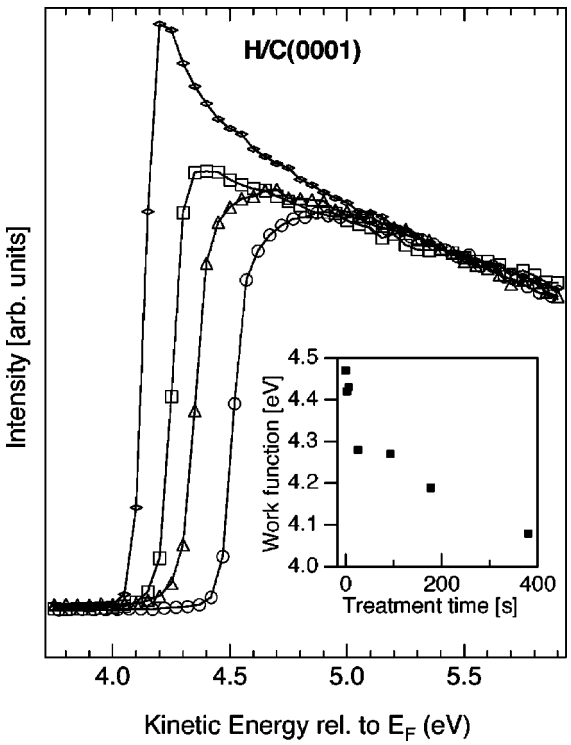

FIG. 7. Low-energy cutoff of the valence band spectra of graphite after different H_2 plasma treatment times. The spectra have been measured using He I (21.2 eV) radiation and an energy resolution of 60 meV. Spectra are given for the untreated surface (circles), 25 s (triangles), 180 s (squares), and 390 s (diamonds) treatment time and are normalized to the intensity at 5.5 eV. The inset shows the work function change as a function of the treatment time.

D. Curvature dependence of H chemisorption

The results discussed above are summarized in Table I. The local curvature is described by the height *h*, which is the distance between a carbon atom and the plane defined by its nearest neighbors. It is as well a measure of the local admixture of sp^3 character. The bond angle varies from 120° (pure sp^2 bonding) to 109.5° for pure sp^3 bonding, i.e., for diamond, which is given here for comparison.[19]

The results obtained for different sp^2-bonded carbon samples reveal a strong dependence of the hydrogen-carbon interaction on the admixture of sp^3 bonding induced by the local curvature of the substrate. The fact that atomic hydrogen adsorbs on SWNT and C_{60}, but not on graphite, indicates a lowered adsorption energy barrier for strongly curved structures. The maximum hydrogen coverage achieved on C_{60} and SWNT upon exposure to atomic hydrogen treatment

TABLE I. Summarized results on the interaction of atomic hydrogen and hydrogen ions with the investigated samples. The height h indicates the distance of a carbon atom to the plane defined by its nearest neighbors and gives a measure for the local curvature of the sp^2 network. $\Delta\phi$ is the maximum reduction of the work function for atomic hydrogen treatments (H) and H_2 plasma treatments (H^+). The ratio (I_π/I_{π_0}) gives the lowering of the intensity on the π-derived states with respect to the untreated sample. The values for the SWNT are for the sample with an average diameter of $d_T = 1.2$ nm. The work function change between the hydrogen-passivated and the hydrogen-free diamond (111) surface is given for comparison (Ref. 19).

	h(Å)	$(I_\pi/I_{\pi_0})_H$	$(I_\pi/I_{\pi_0})_{H^+}$	$\Delta\phi_H$ (eV)	$\Delta\phi_{H^+}$ (eV)
C(0001)(sp^2)	0	1	0.60	0.0	0.4
SWNT	0.11	0.78	0.50	0.3	0.6
C_{60}	0.29	0.53	0.27	0.8	1.3
C(111) (sp^3)	0.52				1.4

is limited by an increase of the adsorption energy barrier to a critical value, as further hydrogen adsorption can be observed by exposure to more energetic hydrogen species of a H_2 plasma. From this consideration the saturation hydrogen coverage upon exposure to atomic hydrogen corresponds to the same critical value of the adsorption energy barrier for C_{60} and SWNT's. That this critical value is obtained at higher hydrogen coverage for C_{60} as compared to the SWNT can have two possible reasons. First, the coverage-dependent energy barrier for the SWNT is offset to higher values as compared to the C_{60}, or second, the energy barrier increases more rapidly with increasing coverage for the SWNT. Considering the DFT results of Sha and Jackson and the fact that no adsorption was observed on planar graphite using atomic hydrogen speaks in favor of a lowered adsorption energy barrier for all coverages when the local curvature in the sp^2 network is increased.

Comparison of the intensity reduction on the π-related features with the lowering of the work function shows a clear dependence between the work function change and the hydrogen coverage, as expected from the coverage dependent dipole density at the surface. However, the lowering of the work function is not proportional to the coverage, but flattens with increasing coverage. This is mainly due to the fact that dipoles depolarize each other with increasing coverage, a phenomena that is generally observed for adsorbates.[30]

It is interesting to compare the work-function changes observed on the sp^2 bonded carbon with experiments done on hydrogen-covered diamond (sp^3). The maximum work function change of 1.3 eV observed on the C_{60} film approaches the values for the diamond C(111) and C(100) surfaces, where the hydrogen-covered surface has a work function that is lowered by 1.4 eV compared to the hydrogen-free surface.[19,29] This gives a further indication of the large dipole created on the the C_{60} film.

IV. SUMMARY AND CONCLUSION

We have studied the interaction of atomic hydrogen and low-energy hydrogen ions with sp^2-bonded carbon surfaces of different local curvatures. Hydrogen chemisorption is evidenced by a reduced intensity on the π-derived states induced by the transformation to more tightly bound σ-derived C-H bond states. The chemisorption of hydrogen generally leads to a lowering of the work function of up to 1.3 eV (C_{60} mulitlayer). This reduced work function is mainly attributed to a modified surface dipole and, by electronegativity arguments, indicates that hydrogen is adsorbed above the carbon layers.

Experiments with atomic hydrogen show that the adsorption energy barrier for bond formation decreases with the local curvature of the sp^2 network since atomic hydrogen was partially adsorbed on C_{60} and SWNT's but not on graphite. This behavior is attributed to the higher sp^3 character of convex sp^2 structures, which is in agreement with DFT calculations[8,9] showing a lowering of the energy barrier for a carbon atom that is raised above the plane defined by its nearest neighbors. Our results show that the adsorption energy barrier increases with increasing coverage, leading to saturation coverages which depend on the form of hydrogen (i.e., atomic or ionic) used for the treatment. Accordingly, we found the highest hydrogen coverage ($\theta \simeq 0.7$) on the C_{60} multilayer using low-energy hydrogen ions.

The experiments indicate a lower estimation of the critical radius of curvature of $r_{cr} \approx 6$ Å for the chemisorption of hydrogen on sp^2-bonded carbon structures. For a more restrictive determination of the critical curvature, SWNT samples with narrow diameter distributions would be required for tube diameters of $d_T > 1.2$ nm.

ACKNOWLEDGMENT

This work was supported by the Swiss National Science Foundation (MaNEP) and the European Network FUNCARS.

*Corresponding author. Email address: pascal.ruffieux@unifr.ch

[1] H.W.Ch. Postma, T. Teepen, Z. Yao, M. Grifoni, and C. Dekker, Science **293**, 76 (2001).
[2] H.J. Choi, J. Ihm, S.G. Louie, and M.L. Cohen, Phys. Rev. Lett. **84**, 2917 (2000).
[3] M. Bockrath, W. Liang, D. Bozovic, J.H. Hafner, C.M. Lieber, M. Tinkham, and H. Park, Science **291**, 283 (2001).
[4] P. Ruffieux, O. Gröning, P. Schwaller, L. Schlapbach, and P. Gröning, Phys. Rev. Lett. **84**, 4910 (2000).
[5] W. Clauss, D.J. Bergeron, M. Freitag, C.L. Kane, E.J. Mele, and A.T. Johnson, Europhys. Lett. **47**, 601 (1999).
[6] Z. Klusek, Appl. Surf. Sci. **125**, 339 (1997).
[7] H.A. Mizes and J.S. Foster, Science **244**, 559 (1989).
[8] L. Jeloica and V. Sidis, Chem. Phys. Lett. **300**, 157 (1999).
[9] X. Sha and B. Jackson, Surf. Sci. **496**, 318 (2002).

[10] S. Nowak, P. Gröning, O.M. Küttel, M. Collaud, and G. Dietler, J. Vac. Sci. Technol. A **10**, 3419 (1992).
[11] O.M. Küttel, J.E. Klemberg-Sapieha, L. Marinu, and M.R. Wertheimer, Thin Solid Films **193/194**, 155 (1990).
[12] U. Bischler and E. Bertel, J. Vac. Sci. Technol. A **11**, 458 (1993).
[13] R.E. Haufler, J.J. Conceicao, L.P.F. Chibante, Y. Chai, N.E. Byrne, S. Flanagan, M.M. Haley, S.C. O'Brien, C. Pan, Z. Xiao, W.E. Billups, M.A. Ciufolini, R.H. Hauge, J.L. Margrave, L.J. Wilson, R.F. Curl, and R.E. Smalley, J. Phys. Chem. **94**, 8634 (1990).
[14] D. Koruga, S. Hameroff, J. Withers, R. Loutfy, and M. Sundareshan, *Fullerene* C_{60}: *History, Physics, Nanobiology, Nanotechnology* (North-Holland, Amsterdam, 1993).
[15] J.L. Martins, N. Troullier, and J.H. Weaver, Chem. Phys. Lett. **180**, 457 (1991).
[16] J. Schäfer, J. Ristein, R. Graupner, L. Ley, U. Stephan, Th. Frauenheim, V.S. Veerasamy, G.A.J. Amaratunga, M. Weiler, and H. Ehrhardt, Phys. Rev. B **53**, 7762 (1996).
[17] J. Robertson and E.P. O'Reilly, Phys. Rev. B **35**, 2946 (1987).
[18] T. Guo and G.E. Scuseria, Chem. Phys. Lett. **191**, 527 (1992).
[19] L. Diederich, O.M. Küttel, P. Aebi, and L. Schlapbach, Surf. Sci. **418**, 219 (1998).
[20] G. Beamson and D. Briggs, *High Resolution XPS of Organic Polymers* (J. Wiley, Chichester, 1992).
[21] J.J. Pireaux, S. Svensson, E. Basilier, P.-A. Malmqvist, U. Gelius, R. Caudano, and K. Siegmann, Phys. Rev. A **14**, 2133 (1976).
[22] R. Graupner, Ph.D. thesis, University of Erlangen-Nürnberg, 1997.
[23] T.R. Ohno, C. Gu, J.H. Weaver, L.P.F. Chibante, and R.E. Smalley, Phys. Rev. B **47**, 13 848 (1993).
[24] L.C. Qin, X. Zhao, K. Hirahara, Y. Miyamoto, Y. Ando, and S. Iijima, Nature (London) **408**, 50 (2000).
[25] H. Kuzmany, W. Planck, M. Hulman, Ch. Kramberger, A. Grüneis, Th. Pichler, H. Peterlik, H. Kataura, and Y. Achiba, Eur. Phys. J. B **22**, 307 (2001).
[26] K. Kobayashi, Phys. Rev. B **48**, 1757 (1993).
[27] S.M. Lee and Y.H. Lee, Appl. Phys. Lett. **76**, 2877 (2000).
[28] S.M. Lee, K.H. An, W.S. Kim, Y.H. Lee, Y.S. Park, G. Seifert, and T. Frauenheim, Synth. Met. **121**, 1189 (2001).
[29] J.B. Cui, J. Ristein, and L. Ley, Phys. Rev. Lett. **81**, 429 (1998).
[30] Gabor A. Somorjai, *Chemistry in Two Dimensions: Surfaces* (Cornell University Press, London, 1981).